I. INTRODUCTION

In many applications such as nondestructive testing, electromagnetic compatibility, identifications, medical diagnosis and etc., we search for sources or anomalies inside an inaccessible regions. This problem classically is done by detection, localization and characterization. The present development of the measurement devices does well in the detection and localization, but the exact determination of the shape, surface and volume reconstruction of the object under consideration are still a problem of paramount importance. Determination of the field distributions from locally measurements outside the source area formulates the inverse electromagnetic problem. The present visualizing devices, high technology methodologies for visualization, image processing and data manipulations give possibilities for precise analysis and solutions of forward and inverse problems in electromagnetics, medicine, architecture etc. Recently, the field theory and image processing techniques were successfully applied for visualization of electromagnetic fields as well as to several inverse electromagnetic problems [1-3].

In this paper we develop a system for modeling and measurement of magnetic field distribution in biological structures caused by the externally applied electromagnetic field. We propose an approach for 3D field reconstruction visualizing the measured data of 2D magnetic field distributions. The finite element method (FEM) is applied for determination of magnetic field distribution in very thin slices of human leg exposed to externally applied time varying magnetic field. The images obtained by visualizing the magnetic field distributions are considered as slices of 3D image. Based on the field theory and image processing techniques, we built 3D reconstruction approach for 3D visualization of magnetic field. The proposed approach was successfully applied for 3D reconstruction and visualization of magnetic field and current distributions. This approach suggests a possibility for 3D visualization of magnetic field with complex structure and characteristics.

During modeling, simulation and measurements usually very large multidimensional datasets are generated and utilized. In order to facilitate the analysis of the phenomena, processes as well as magnetic field distribution in biological structures during magnetic stimulation the virtual biomagnetic microscope is developed.

determined by the Biot-Savart law

$$\mathbf{B} = \frac{\mu_0}{4\pi} I(t) \int_S \frac{\mathbf{dl}(\mathbf{r}') \times (\mathbf{r} - \mathbf{r}')}{|\mathbf{r} - \mathbf{r}'|^3}, \tag{2}$$

where μ_0 is the permeability of free space.

The electric field is expressed by magnetic vector potential **A** and electric potential V as

$$\mathbf{E} = -\frac{\partial A}{\partial t} - \nabla V. \tag{3}$$

The magnetic field distribution changes according to respective configuration of electromagnetic systems used to excite the magnetic field in human body.

Development of computation model of magnetic field distributions that take into account all properties and characteristics of the biological structures are extremely important in order to realize effective medical diagnosis and therapy. The numerical methods, e.g. finite element method and boundary element method, are powerful tools to investigate the electric and magnetic field distribution produced by electromagnetic devices. Numerical techniques are capable of analysis of various heterogeneous structures of biological bodies exposed to magnetic fields.

III. MAGNETIC STIMULATION OF HUMAN BODY

The human leg has been exposed to magnetic field excited by coil. The cross-section of the human anatomical leg regions under consideration is shown in Fig. 1(a). The images of the slices with distance 1 cm between them are presented in Fig. 2. A three-dimentional stacked image model in Fig. 1(b) is created from the 2-D slices shown in Fig.2.

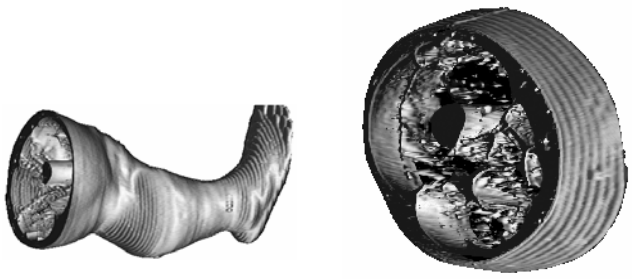

(a) (b)

Figure 1. Cross section of human leg.

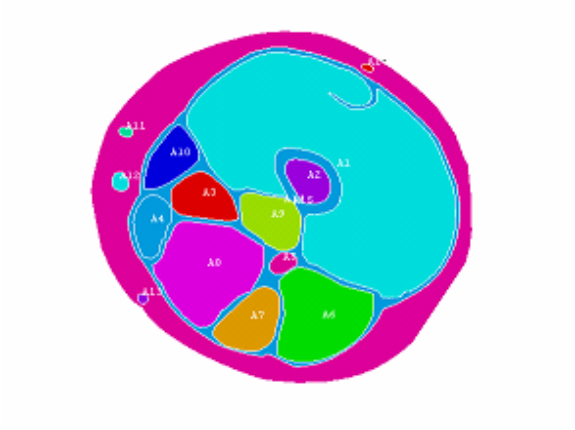

Figure 4. Finite element model areas

Table 1 Tissue properties and model areas

Tissue	Areas	Conductivity σ, S/m
Blood	1,9,11	7.00 e-01
Bone	5	2.03 e-02
Bone marrow	26	8.51 e-01
Fat	24	2.34 e-02
Muscle	2,4,7,8,10,12,15,16,17,18,19	3.34 e-01
Nerve	5	3.20 e-01
White matter	6	6.55 e-02
Skin dermis	25	2.01 e-02

The leg slices are with diameter of 20 cm approximately and length of 1 cm. The slice images are traced and the corresponding areas and volumes for application of FEM are created as shown in Fig. 4. The tissue properties used in the FEM model are listed in Table 1. The medium is accepted to be magnetically homogeneous, with relative magnetic permeability $\mu_r = \mu_0$.

field distribution is determined in the slice. Using the developed FEM model the magnetic field was calculated and visualized for each slice of the human leg during magnetic stimulation. The field distribution is investigated at different values of coil current and frequencies. The results presented are for the peak value of the current 1kA with frequency 10 kHz. The magnetic field distributions are visualized and presented in Fig. 5. Figure 6 shows the current distributions caused by the induced voltage.

V. 3D RECONSTRUCTION OF MAGNETIC FIELD

A 3D volume of data for visualization of magnetic field was created from the 2D slices of locally determined and visualized magnetic field distribution at parallel surfaces by transforming each pixel in the 2D slice to its corresponding 3D location using the position, orientation and Green's function. If the 2D slices are arbitrary oriented and positioned in space, some of the voxels in the volume data set are not assigned intensity values. These voxels were identified and assigned an intensity value based on the weighted average of its neighboring voxels. Consequently resembled 3D magnetic field data set is visualized.

(a) Upper part (b) Lower part

Figure 7. 3D reconstruction of magnetic field distributions

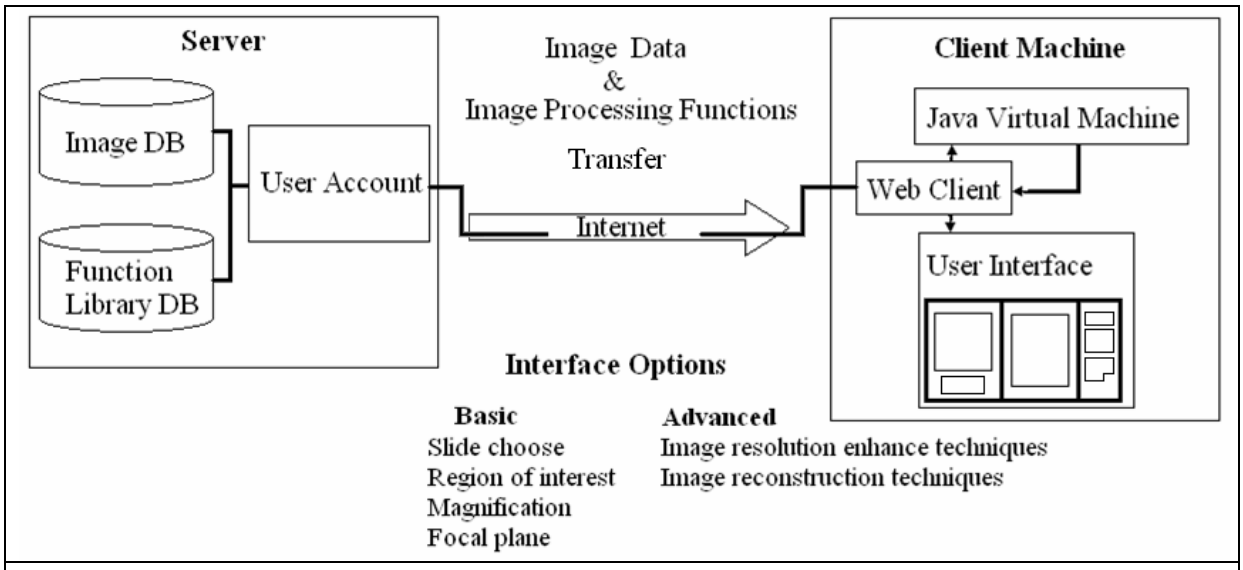

Figure 9 Basic architecture of the virtual microscope

The 3D virtual microscope interface shown in Fig. 11 consists of 3D anatomy display window, the 3D field distribution window and control window. The 3D biological display window shows the 3D reconstruction of the available biological slices of the object under consideration. The 3D Field Distribution window shows the 3D field distribution of the object obtained by reconstruction of 2D field distribution presented by 2D virtual biomagnetic microscope interface shown in Fig. 10.

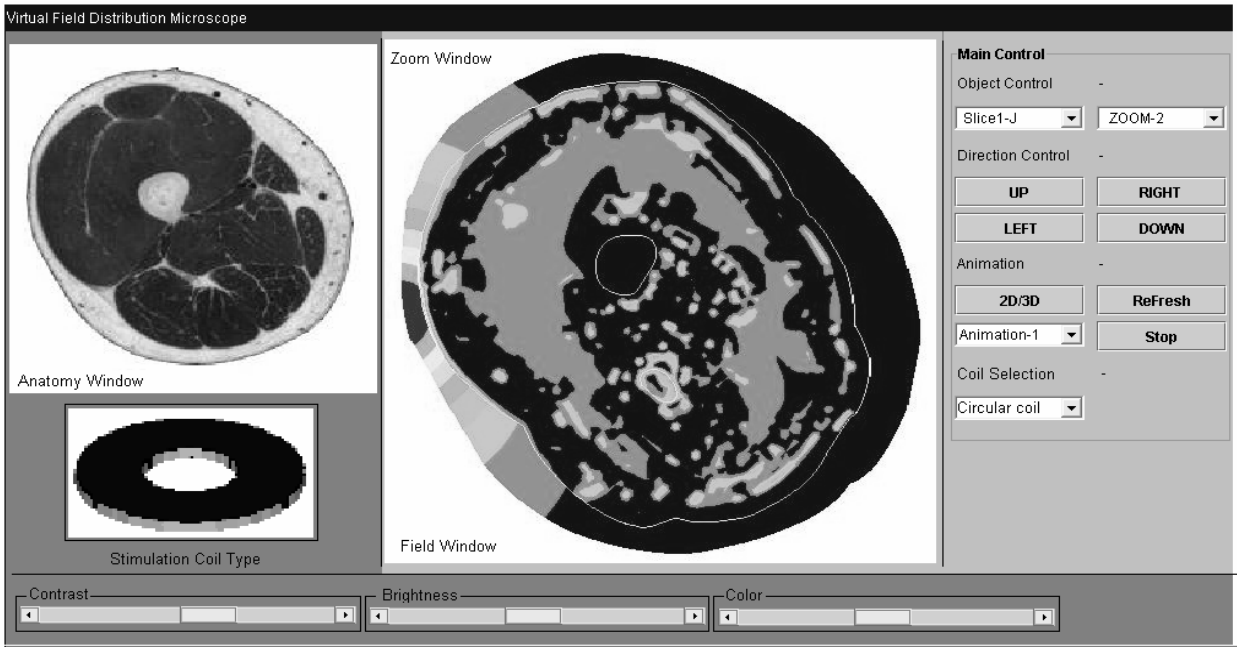

Figure. 10. 2D Virtual microscope interface

field. Design of a two-dimensional array with 8 sensors is shown in Fig.14. This type of sensor can assure simultaneously information of two components of magnetic field flux density components (X-Y).

Several types for sensor signal pick up circuit systems are considered in Fig. 15-17.

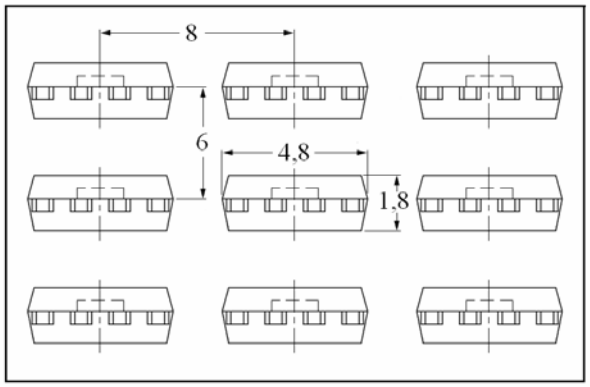

Fig.12. 3x3-element square array.

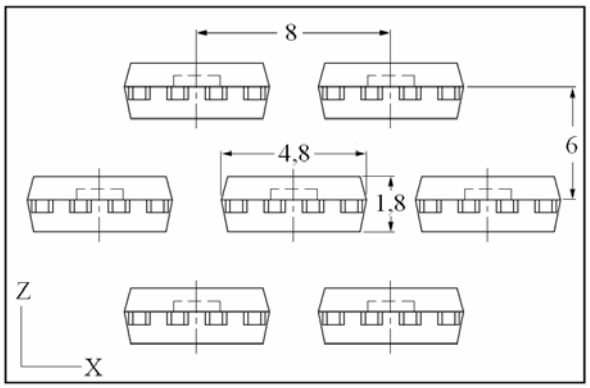

Fig.13. 7-element hexagonal array.

First array circuit in Fig.14 is based on National Instruments USB-6008 data acquisition device. Voltage range of USB-6008 is 10V at resolution 14,7mV with accuracy ±(1,7%)[20]. Limitation of this circuit is the number of analog input channels of data acquisition device.

Second array circuit in Fig.15 uses multiplexing IC controlled by a signal generator. Pick-up voltage signal is measured with Protek-506 Digital multimeter with voltage range 400mV at resolution 0,1mV with accuracy ±(1,5%) [21].

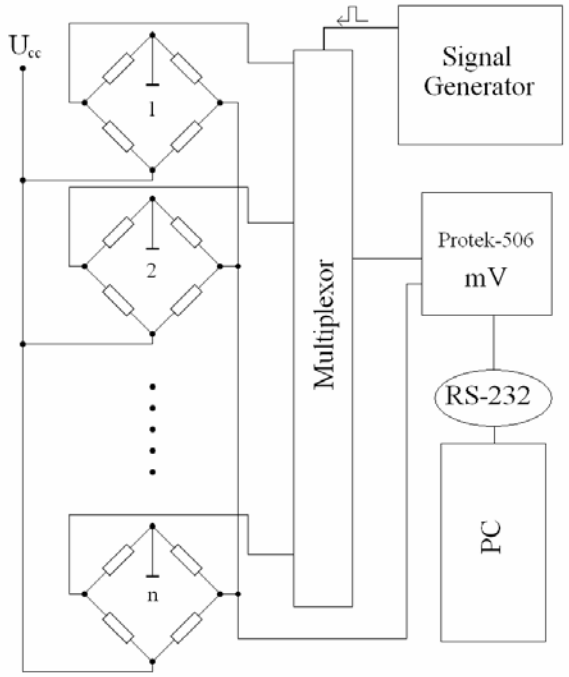

Fig.16. Signal pick-up circuit with Protek506.

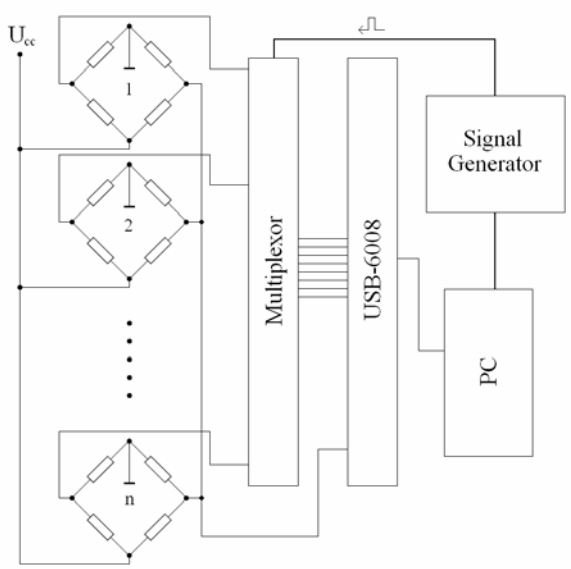

Figure17. Signal pick-up circuit.

Multiplexer in Fig. 17 activates eight pick-up AMR sensors at the time. The receiving configuration may be composed up to 64 sensor elements. Eight channels are activated in eight acquisition time intervals (or time slots of DAQ) to activate the complete probe in a very short period of time.

REFERENCES

[1] I. Marinova, H. Endo, S. Hayano, and Y. Saito, “Image Reconstruction for Electromagnetic Field Visualization by an Inverse Problem Solution”, *Int. Journal of Applied Electromagnetics and Mechanics*, 15 IOS Press, (2001/2002), pp. 403-408.

[2] I. Marinova, H. Endo, S. Hayano, and Y. Saito, “Inverse Electromagnetic Problems by Field Visualization”, *IEEE Trans. Magn*. Vol. 40, No. 2, 2004, pp.1088-1093

[3] T. Doi, S. Hayano, I. Marinova, and Y. Saito, “Defect recognition in conductive materials by local magnetic field measurement”, *Journal of Applied Physics*, Vol. 75, No. 10, 1994, pp. 5907-5909

[4] I. Marinova, C. Panchev, and D. Katsakos, “A Neural Network Inversion Approach for Electromagnetic Device Design”, IEEE. Trans. Magn, Vol. 36, No. 4, 2000, pp. 1080-1084

[5] I. Marinova, C. Panchev, and D. Katsakos, “Gradient Coil Design for MRI by Neural Networks”, The Joint Seminar’99, Nov. 1-3, Sapporo, Japan, 1999, pp.14-15

[6] C. Im, C. Lee, “Computer-Aided Performance Evaluation of a Multichanel Transcranial Magnetic Stimulation System”, *IEEE Trans. Mag*n., Vol. 42, No. 12, 2006, pp. 3803-3808

[7] I. Marinova and L. Kovachev, “Inverse Approach for Determination of the Coils Location in Magnetic Stimulation”, in Applied Electromagnetics. Proceedings of the 3rd JBMSAEM, Sept. 15-17, Ohrid, Macedonia, 2000, pp. 140-146

[8] V. Krasteva , S. Papazov and I. Daskalov, “Magnetic Stimulation for Non-homogeneous Biological Structures”, *BioMed Eng OnLine*. 1: 3, http://www.biomedical-engineering-online.com/content/1/1/3, 2002

[9] P. Basser, ”Focal Magnetic Stimulation of an Axon”, IEEE Trans. Biomedical Engineering, Vol. 41, No. 6, 1994)

[10] S. Ueno, “Inverse Problem Aspects in the Field of Biomagnetic Applications”, Non-Linear Electro- magnetic System. V. Kose and J. Sievert (Eds.) IOS Press, 1998

[11] R. Jalinous, “Guide to Magnetic Stimulation”, Magstim Company Ltd., 1998

[12] M. A. Stuchly, “Applications of Time-varying Magnetic Fields in Medicine”, *Critical Review in Biomedical Engineering*, Vol. 18, No. 2, 1990, pp. 89-124

[13] J. P. Reilly, “Peripheral Nerve Stimulation by Induced Electric Currents: Exposure to Time Varying Magnetic Fields”, *Medical & Biological Engineering & Computing*, 1998, pp. 101-118